Journal of Fluorine Chemistry 191 (2016) 29–41

Contents lists available at ScienceDirect

Journal of Fluorine Chemistry

journal homepage: www.elsevier.com/locate/fluor

Fluoro-curcuminoids and curcuminoid-BF_2 adducts: Synthesis, X-ray structures, bioassay, and computational/docking study

Kenneth K. Laali[a,*], Benjamin M. Rathman[a], Scott D. Bunge[b], Xin Qi[c], Gabriela L. Borosky[d]

[a] Department of Chemistry, University of North Florida, 1 UNF Drive, Jacksonville, FL 32224, USA
[b] Department of Chemistry and Biochemistry, Kent State University, Kent, OH 44242, USA
[c] Department of Medicinal Chemistry, College of Pharmacy, University of Florida, P.O. Box 100484, Gainesville, FL 32610, USA
[d] INFIQC, CONICET and Departamento de Matemática y Física, Facultad de Ciencias Químicas, Universidad Nacional de Córdoba, Ciudad Universitaria, Córdoba 5000, Argentina

ARTICLE INFO

Article history:
Received 30 August 2016
Received in revised form 15 September 2016
Accepted 16 September 2016
Available online 17 September 2016

Keywords:
Fluorocurcuminoids
Curcuminoid-BF_2 adducts
Synthesis
X-ray analysis
In-vitro bioassay
Computational docking

ABSTRACT

A series of α-carbonyl fluorinated curcuminoids were synthesized by direct mono- and difluorination with Selectfluor (F-TEDA-BF_4) at r.t. without using a base or additive. Ring fluorinated/trifluoromethylated curcuminoid-BF_2 adducts were synthesized by reaction of the corresponding benzaldehydes with acetylacetone-BF_2. Decomplexation of CUR-BF_2 adducts under microwave irradiation gave the corresponding curcuminoids. Multinuclear NMR and X-ray analysis confirm that curcuminoids bearing fluorines or trifluoromethyl groups in the aryl rings as well as those that are monofluorinated at the active methylene position all exist as enol tautomers. The α,α-difluorination brings about significant conformational change as these curcuminoids become fixed in the 1,3-diketone configuration. The X-ray structures of CUR-BF_2 complexes are consistent with the formation of symmetrical adducts with equal B—O bond distances. The anti-proliferative activity of these compounds were tested by *in-vitro* bioassay against several different cancer cell lines. The corresponding CUR-BF_2 adducts exhibited exceptionally high activities at micromolar and in some cases nanomolar concentrations that greatly surpass the activity of parent curcumin. Computational docking calculations were performed to gauge binding energies of these compounds in HER2 protein, and in 20S proteasome, for comparison with the bioassay-derived activity data.

1. Introduction

Curcumin (CUR) **1** is a non-toxic natural product extracted from *turmeric* and has been used for centuries as dietary supplement and therapeutic agent in Chinese and Asian medicines. Extensive studies have shown that curcumin possesses anti-carcinogenic effects on various types of cancer, as well as anti-inflammatory, anti-oxidant and other properties that are beneficial to human health and cancer prevention [1–3]. The central core of CUR molecule is a conjugated 1,3-diketone that exits almost exclusively as the enol-tautomer (Fig. 1).

Despite a relatively simple molecular structure, curcumin has a combination of features that provide several favorable binding sites/modes, namely hydrophobic phenyl domains (potential sites for π–π interaction with the aromatic side chains in aminoacids), the phenolic OH groups (hydrogen bonding interactions), and the central β-keto-enolic moiety (participate in H-bonding, chelate metal cations, and act as Michael acceptor). These favorable features give curcumin a unique ability to interact with target proteins.

In spite of these attributes a major obstacle toward the development of CUR-derived cancer drugs is its rapid metabolism and poor water solubility. In order to overcome these drawbacks the synthetic/medicinal chemistry community has devoted significant effort to modify the CUR structure by synthesizing analogs that might circumvent these limitations, especially with regard to metabolic instability.

Whereas the conjugated 1,3-diketone moiety is considered to be very important in interaction with target proteins [1], it is believed that this region contributes to its low metabolic stability. Therefore much research effort has been devoted to structural modifications with the goal to replace the central portion of the molecule with metabolically more robust polar moieties.

* Corresponding author.
E-mail address: Kenneth.Laali@UNF.edu (K.K. Laali).

http://dx.doi.org/10.1016/j.jfluchem.2016.09.009
0022-1139/

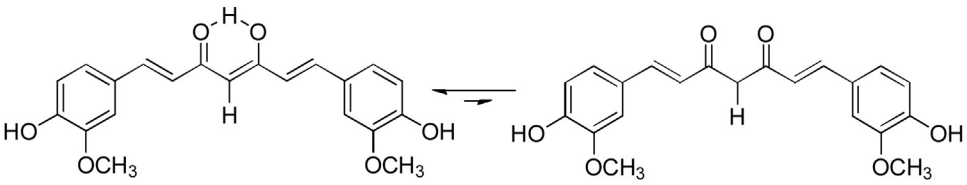

Fig. 1. Tautomerism in curcumin – exclusive presence of the enol tautomer.

These structural modifications have included introduction of enaminone, oxime, and dienone, and replacement of the central moiety with pyrazole and isoxazole rings [4–9]. It is noteworthy that many of these synthetic modifications represent significant departure from CUR's original skeleton. Other studies have reported improved bioactivity by transforming the phenolic OH in CUR to acetates and aminoacid conjugates [10], cinnamic and succinyl esters [11,12], other types of esters [13], and acetamides [14]. Introduction of ester or α,β-unsaturated ester linkers into the active methylene region has been used to prepare curcuminoid libraries as potential antitumor agents for lung and prostate cancer [15–17]. Encapsulation or conjugation with nanoparticles, polymeric micelles, or liposomes have been explored as a way to deliver curcuminoids to cancer cells [3].

Selective fluorine introduction into pharmaceuticals is a powerful strategy for improving metabolic stability and physiochemical properties [18,19], but this approach has remained greatly under-utilized with respect to curcuminoids.

Since the standard approach for the assembly of symmetrical CUR analogs is via a "double aldol" condensation of aldehydes with

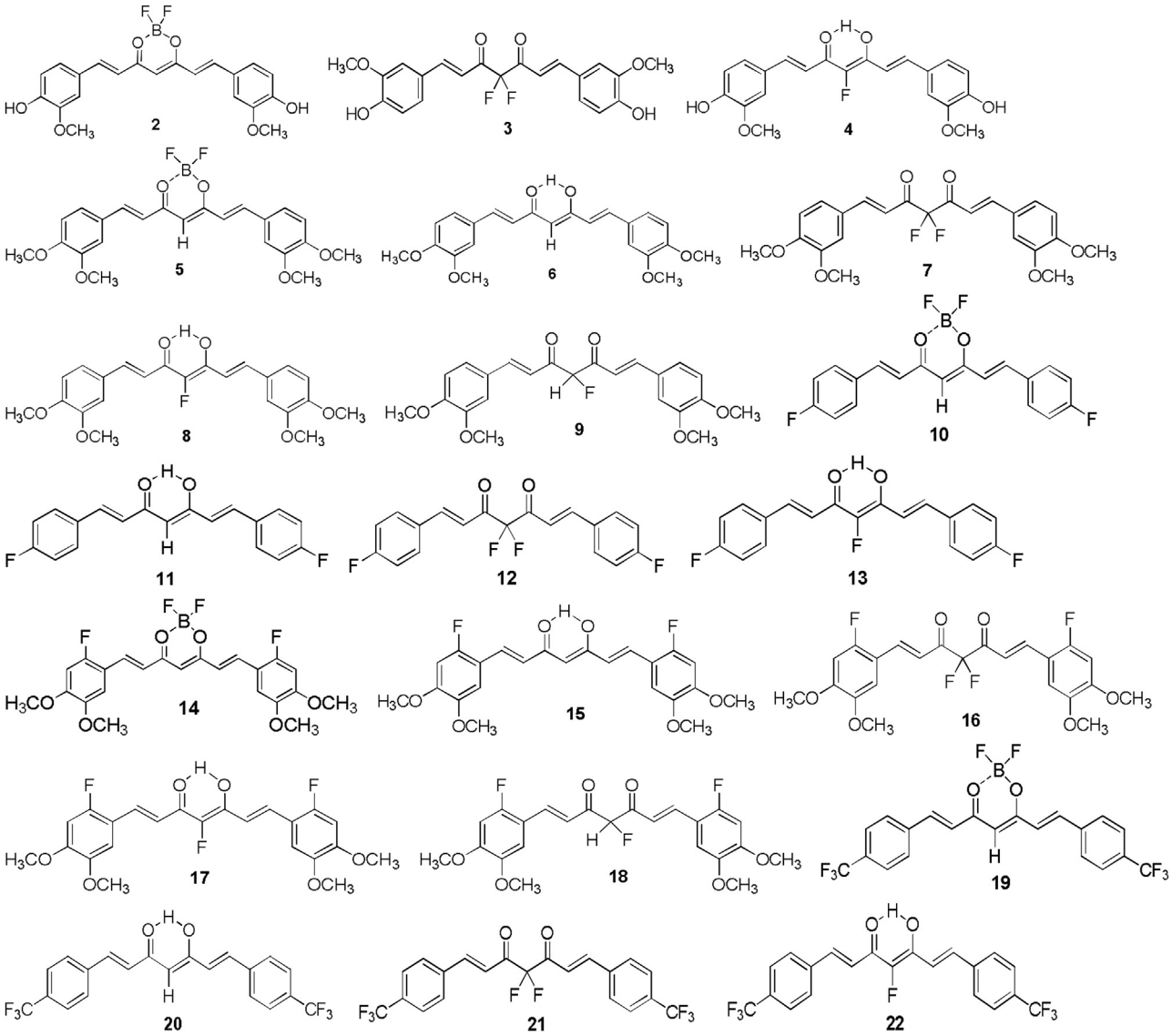

Fig. 2. Compound sheet.

acetylacetone [20,21], ring fluorinated derivatives can be synthesized via this route, however very few examples have been reported, and with limited NMR data [22].

To the best of our knowledge only two examples of curcuminoids bearing a single fluorine at the active methylene position (along with an ester linker or a methyl group) have been reported [16,17]. The reported methods required additional steps, namely deprotonation (NaH/DMF) followed by fluorination, as well as additional steps for protection and deprotection of the phenolic OH in the case of parent CUR.

Considering the importance of the 1,3-diketo moiety in the CUR skeleton for interaction with target proteins, development of methods for direct fluorine introduction into the active methylene position is highly desirable, but no such methods have hitherto been reported.

It is also noteworthy that despite extensive bioassay studies on curcuminoids [1–3], the potential of CUR-BF_2 complexes as anti-proliferation agents has remained largely unexplored. Review of the published literature shows that these compounds are usually treated as "intermediates" en-route to curcuminoids, and only few examples exist in which they have been characterized, albeit with limited NMR data [20], except in two independent recent studies [23], where a series of CUR-BF_2 complexes bearing various donor end-groups were synthesized and their photophysical properties were explored.

Inspired by our earlier fluorination study of carbonyl compound [24], we report here the synthesis of novel curcuminoids that are mono- and difluorinated at the active methylene position by direct one-pot fluorination with Selectfluor (F-TEDA-BF_4) without using a base or additive (see Fig. 2). In addition to parent CUR (**1**) and its symmetrical O-dimethylated analog (DMC; **6**), symmetrical curcuminoids bearing fluorines (**11** and **15**) and trifluoromethyl groups (**20**) in the phenyl rings were also synthesized, and subsequently mono- and difluorinated at the active methylene position (see Fig. 2). The corresponding curcuminoid-BF_2 adducts which serve as synthetic intermediates en-route to these curcuminoids were isolated and characterized. The X-ray crystal structures were obtained for CUR-BF_2 adducts **5**, **10**, and **14**, and for the F-CUR **8**. The cell growth inhibitory and apoptosis inducing effects of these compounds were examined by *in-vitro* assays against leukemia (MOLT-4), prostate cancer (PC3 and LNCap), as well as lung (A549) and breast cancer (MDA231) cell lines. A selected group of compounds were screened by the NCI 60 cell panel. Computational docking studies were also performed on CUR-BF_2 adducts and fluorinated curcuminoids to compare their binding energies in HER2 protein relative to a well-known ligand (SYR), versus trends from bioactivity data for breast cancer (IC_{50} MDA231), and in proteasome in comparison with bioassay data in leukemia (IC_{50} MOLT-4).

2. Results and discussion

2.1. Direct fluorination of parent curcumin 1

Preliminary feasibility studies were performed to identify suitable solvents for the reaction of **1** with Selectfluor. Experiments were performed by using 0.1 mmol of CUR and 1.1 and 2.1 equivalents of Selectfluor, and the progress of the reactions were monitored by ^{19}F NMR (and by TLC). ^{19}F NMR provided a convenient and direct method to gauge chemoselectivity in different solvents. Apart from F-CUR and F_2-CUR, formation of CUR-BF_2 adduct was observed in some solvents, notably in water and in acetone under microwave irradiation (more in Section 2.2). Presence of a distinct doublet at δ −195 ppm (J_{HF} = 50 Hz) signified the 1,3-diketo-tautomer of F-CUR present in different proportions in some solvents. Application of microwave (MW) increased the proportion of CUR-BF_2 adduct in acetone as solvent (Table 1).

Based on these studies, MeOH was selected as solvent of choice for direct difluorination of curcuminoids, whereas MeCN was chosen for monofluorination.

To minimize the formation of other species observed in ^{19}F monitoring study in MeCN solvent, the monofluorinations were performed at 0 °C and continued at r.t. A noteworthy feature in these studies was that competing ring fluorination products were not detected, and further fluorination beyond the formation of F_2-CUR was not observed in a control experiment using excess Selectfluor (4 equiv.). Based on these studies compounds **3** and **4** were synthesized and isolated according to Fig. 3.

2.2. Development of a general and improved synthetic method for the assembly of the curcuminoid skeleton

The base-catalyzed "double aldol" condensation of aldehydes with acetyl acetone serves as a standard method to assemble the curcumin skeleton. Earlier methods employing boric oxide or boric acid as additive had drawbacks with respect to reproducibility, and a more reliable method involving the reaction of acetylacetone-BF_2 complex with aldehydes followed by hydrolysis of the complex was developed [20]. Microwave-assisted one-pot methods that

Table 1
^{19}F NMR monitoring of solvent effect on fluorination selectivity[a].

Solvent[b,c]	^{19}F NMR signal at −115 ppm (s) F_2-CUR	^{19}F NMR signal at −140 ppm (s) CUR-BF_2	^{19}F NMR signal at −176 ppm (s) F-CUR	^{19}F NMR signal at −195 ppm (d) Diketo-tautomer of F-CUR
Acetonitrile/r.t.[d]	–	11%	55%	34%
Methanol/r.t.[e]	100%	–	–	–
Ethanol/reflux[d]	61%	33%	6%	–
DMF/reflux[d]	21%	–	43%	36%
THF/r.t.[d]	24%	27%	32%	17%
THF/MW[d]	15%	36%	24%	25%
Acetone/r.t.[e]	66%	3%	23%	8%
Acetone/MW[d]	24%	64%	6%	6%
Water/reflux[e]	–	100%	–	–

[a] Reported percentages are based on relative integrals of these species in ^{19}F NMR (not taking into account signals due to unreacted Selectfluor and its byproducts).
[b] R.T. reactions were allowed to run overnight and reflux temperature was limited to 70 °C.
[c] MW conditions: 200 W until temperature reached 140 °C.
[d] Selectfluor (1.1 equiv.).
[e] Selectfluor (2.1 equiv.).

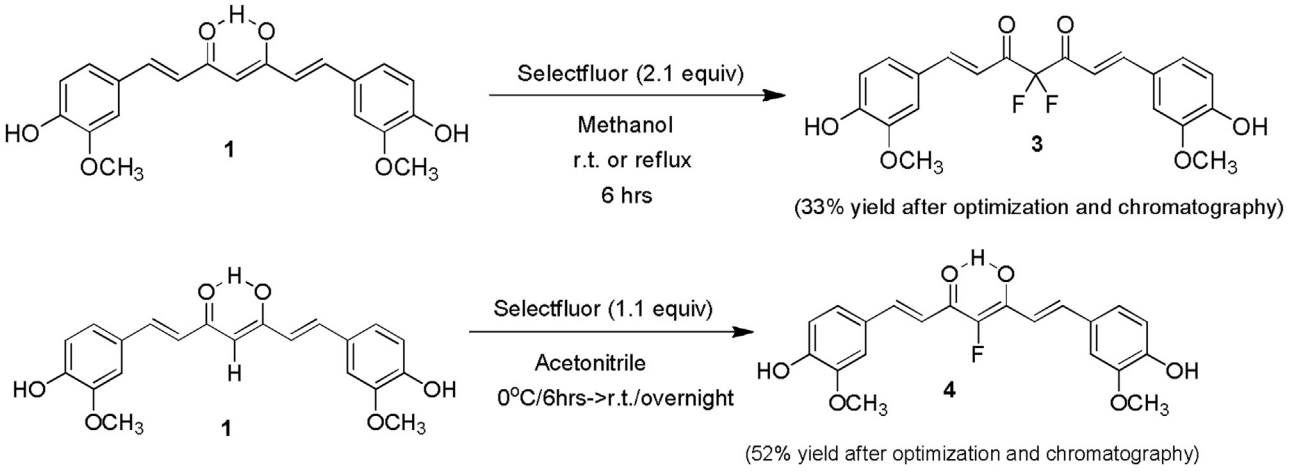

Fig. 3. Synthesis and isolation of F_2-CUR (**3**) and F-CUR (**4**).

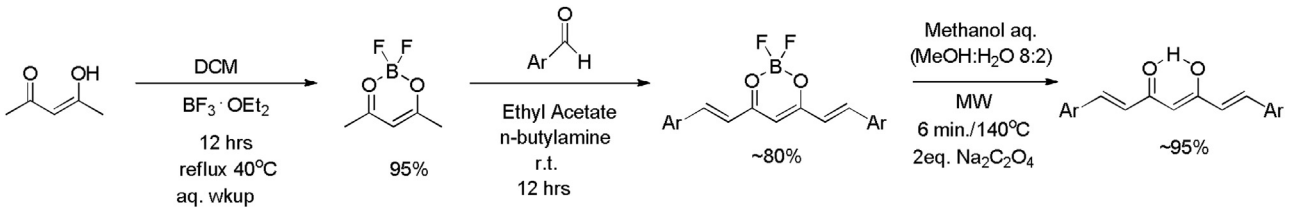

Scheme 1. Synthetic sequence for the preparation of CUR-BF_2 compounds and curcuminoids.

employed calcium oxide, and boric acid/sodium sulfate as additives in toluene solvent had also been reported [21,25].

In the present study, we found the reported hydrolytic/decomplexation process involving multiple steps [20] to be inefficient. Instead, the curcuminoid-BF_2 adducts and their corresponding curcuminoids were synthesized as outlined in Scheme 1. A microwave-assisted method reported for decomplexation of curcumin-quinolone hybrids [26] was adopted but modified by addition of sodium oxalate. Sodium oxalate serves as a bidentate ligand and chelating agent to preferentially coordinate

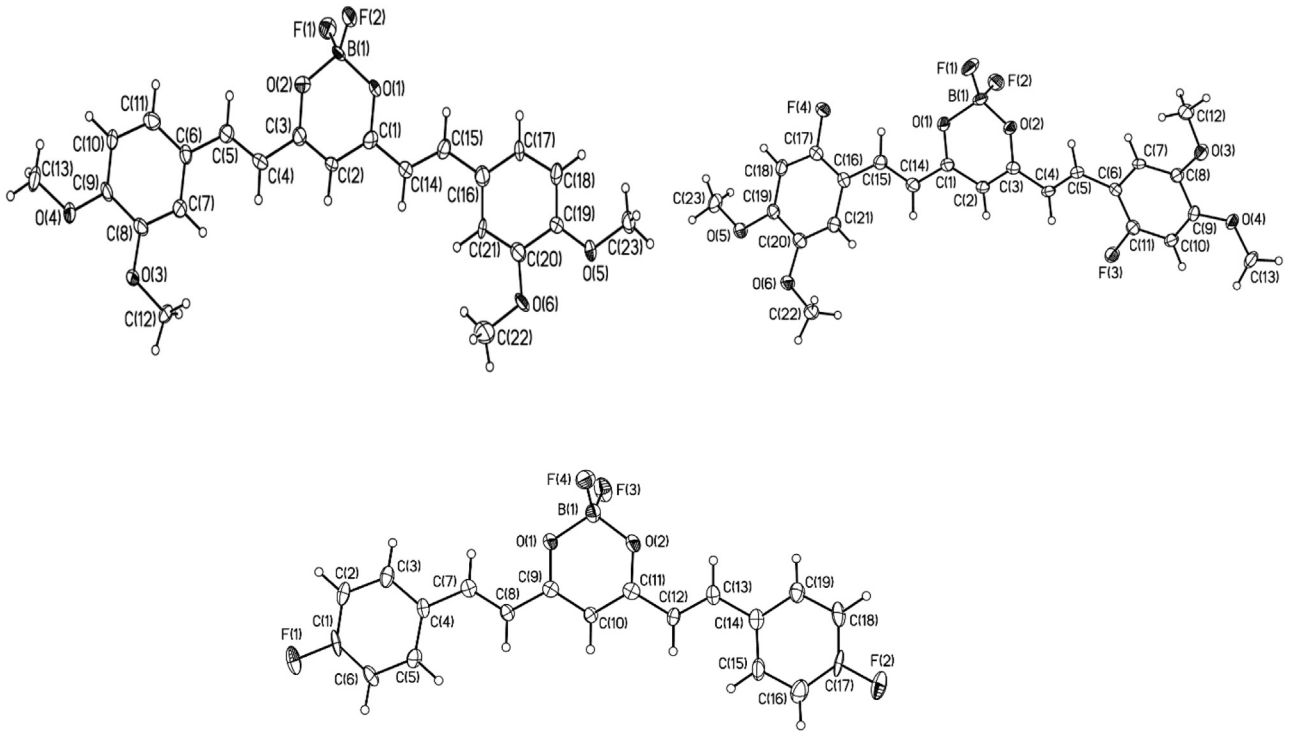

Fig. 4. X-ray structure of CUR-BF_2 adducts **5, 14,** and **10.**

with BF_2, possibly forming sodium-difluoro(oxalato)borate which is a known compound [27].

In initial studies of solvent effect on fluorination selectivity using Selectfluor (Table 1), formation of curcumin-BF_2 adduct was unexpectedly observed under microwave irradiation in acetone or in water. Whereas the method represents an interesting alternative for the synthesis of CUR-BF_2 adducts, in practice the isolated yields of this MW-assisted method were lower (see experimental) as compared to the method outlined in Scheme 1, and it was therefore not used in subsequent reactions.

By using the method outlined in Scheme 1, symmetrical curcuminoids **6**, **11**, **15**, and **20** were synthesized (see Fig. 2). As with parent **1**, these curcuminoids are also exclusively present in the enolic form (NMR). In addition, the corresponding CUR-BF_2 adducts **5**, **10**, **14**, and **19** (Fig. 2) were isolated in high yields and fully characterized (see exp. section).

The X-ray structures for CUR-BF_2 adducts **5**, **10**, and **14** (Fig. 4, and Supplementary data), confirm the symmetrical coordination of BF_2 to the two oxygens in the enolic configuration. The asymmetric unit in CUR-BF_2 **5** corresponds to one molecule with a total of four molecules in each cell. Each molecule interacts with an adjacent molecule via one H–F contact. A packing diagram is shown in Fig. 5 (see Supplementary data for additional information).

Whereas attempts to obtain X-ray quality crystals for the bis-trifluoromethyl-CUR-BF_2 adduct **19** were unsuccessful, its DFT-optimized structure (Fig. 6) fully agrees with a symmetrically BF_2-coordinated adduct.

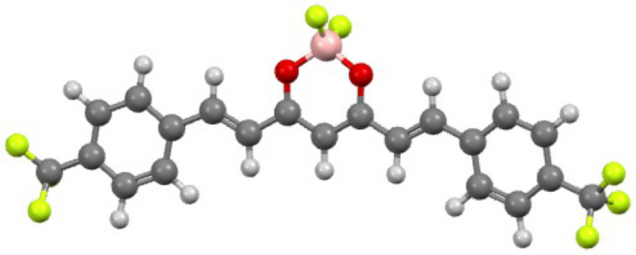

Fig. 6. Optimized structure of $(CF_3)_2$-CUR-BF_2 **19** by B3LYP/6-311 + G(d,p).

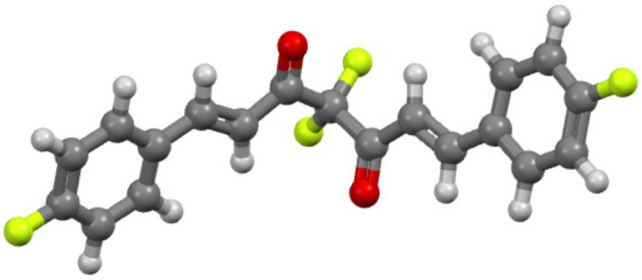

Fig. 7. Optimized structure of **12** by B3LYP/6-311 + G(d,p).

2.3. Synthesis of α-carbonyl fluorinated curcuminoids and structural features

The corresponding α-carbonyl difluorinated analogs (**7**, **12**, **16**, and **21**) were synthesized in good to moderate isolated yields by using 2.1 equivalents of Selectfluor, following the same procedure applied to fluorination of parent **1** (Fig. 1). These compounds exhibit distinctive two-bond C/F coupling with the carbonyls, giving rise to a ~28 Hz triplet in ^{13}C NMR (see Experimental). The DFT optimized structure of tetrafluorinated curcuminoid **12** (Fig. 7) shows notable conformational changes resulting from tautomerization.

The α-carbonyl monofluorinated analogs (**8**, **13**, **17**, and **22**) were synthesized by reaction with 1.1 equivalent of Selectfluor in MeCN (analogous to synthesis of **4;** Fig. 3). Concomitant formation of the difluorinated analogs was observed in the crude reaction mixtures in the monofluorination reactions, which could be minimized by running the reactions initially at 0 °C, then warming to r.t. and continuing to stir at room temperature.

The α-carbonyl monofluorinated compounds exhibit a distinctive two-bond C/F coupling with the carbonyls, giving rise to a 20–23 Hz doublet in ^{13}C NMR. The 1,3-diketone tautomer can be readily recognized by the presence of a ~50 Hz doublet in ^{19}F and ^{1}H NMR due to geminal H/F coupling (see experimental).

Whereas the monofluorinated curcuminoids **4**, **13**, **17**, and **22** are exclusively present in the enolic form, compound **8** was present as a 75:25 (enol to ketone) tautomeric mixture (by ^{19}F NMR).

Interestingly, the X-ray structure of **8** shows only the enolic tautomer and exhibits intramolecular hydrogen bonding and one H-F contact with a distance of 2.44 Å (Fig. 8).

The asymmetric unit for **8** corresponds to three crystallographically nonequivalent molecules with a total of six molecules in each unit cell (see Supplementary data for more detail).

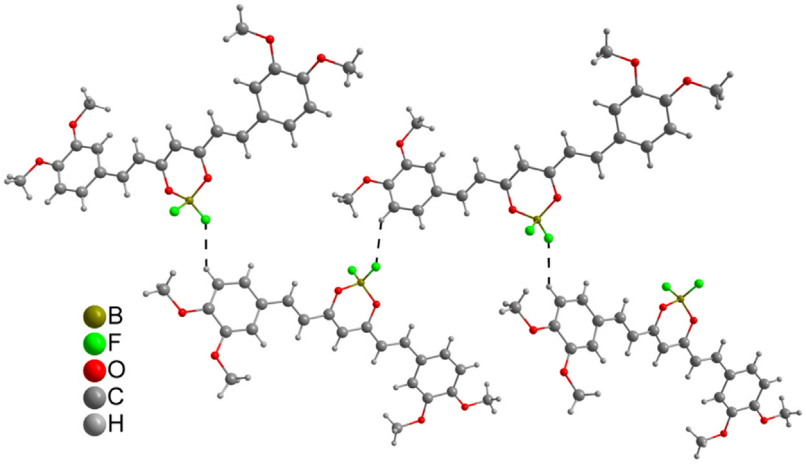

Fig. 5. Crystal packing diagram of **5**.

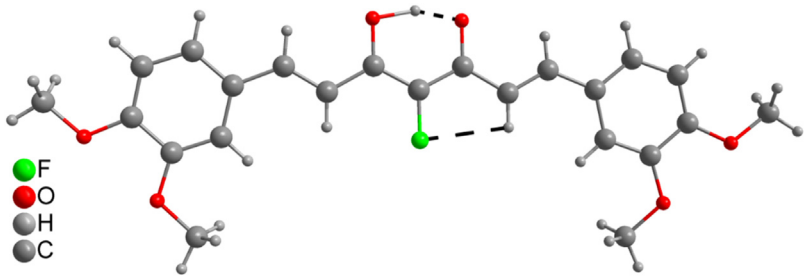

Fig. 8. Ball and stick plot of **8**.

A notable feature in the X-ray crystallographic data is absence of any significant

π–π stacking. Intermolecular interactions appear to be predominantly through short H-F contacts.

2.4. Cell growth inhibitory effects against human cancer cells – bioassay

To evaluate the cell growth inhibitory and apoptosis inducing effects of the fluorinated curcuminoids and their BF_2 adducts, *in-vitro* bioassay tests were performed on four different cancer cell lines namely: MOLT-4 (human leukemia suspension cancer cell line), PC3 and LNCap (human androgen sensitive and insensitive prostate cancer cell lines respectively), A549 (lung cancer), and MDA231 (breast cancer), and the results are sketched in Table 2.

Based on the magnitude of IC_{50} values (Table 2), compounds **5**, **6**, **8, 10** and **14** (Fig. 9) exhibited high potencies toward multiple cancer cell lines, with measured activities at low micro-molar concentrations, and in the case of compound **5** in nano-molar concentration for leukemia.

These anti-proliferative activity trends far exceed those of parent curcumin. It is noteworthy that three of these compounds are CUR-BF_2 adducts.

Comparing the IC_{50} data for compound **6** with the α-carbonyl-monofluorinated analog **8** indicates increased activity as a result fluorine introduction, notably against breast cancer. Compound **6** (DMC) was previously tested as an anti-prostate cancer agent.[17] The reported IC_{50} values against PC3 and LNCap are near identical to those in the present study. Some of the other fluorinated curcuminoids were also more active than their precursors, in particular against leukemia. The α-carbonyl-difluorinated analogs **3** and **12** exhibited increased potency (against MOLT-4) as compared to their curcuminoid precursors **1** and **11.** Overall, except for compound **11** which exhibited lower activity relative to curcumin, all others were more active than parent curcumin, but those shown in Fig. 9 were clearly superior.

The CUR-BF_2 adducts **5**, **10**, and **19**, and the bis-trifluoromethyl-CUR **20** and its difluoro-derivative **21** were screened at the National Cancer Institute using NCI-60 cell one-dose protocol (10^{-5} M). Compounds **10**, **19**, **20**, and **21** exhibited relatively modest growth inhibition activities (10–20%) that were below the NCI's threshold criteria for further testing. The CUR-BF_2 adduct **5** on the other hand proved highly active, with growth inhibition 70%-80% and cell death up to 33%, and has been selected by NCI for further testing.

2.5. Computational docking study

In an effort to shed some light on the factors determining the bioactivity of these curcumin analogues, molecular docking calculations were performed in the active site of HER2. Human epidermal growth factor receptor 2 (HER2) is one of the tyrosine kinase receptors in EGFR family, which is known to play a central role in the pathogenesis of several human cancers [28]. Amplification or overexpression of HER2 occurs in breast, prostate, gastric/gastroesophageal, ovarian, endometrium, bladder, lung, colon, and head and neck cancers. Therefore, it is a drug target for cancer therapy focusing on inhibiting HER2 to reduce tumor growth [28]. Taking this into account, binding energies in HER2 were compared

Table 2
In vitro cell viability bioassay[≠].

	Leukemia IC_{50} (μM)[a,b]	Prostate Cancer IC_{50} (μM)[a,c]		Lung Cancer IC_{50} (μM)[a,c]	Breast Cancer IC_{50} (μM)[a,c]
Curcuminoid	MOLT-4	PC3	LNCap	A549	MDA231
Parent 1	19	9.0	9.7	18.0	11.5
4	3.6*	7.4	13.0	20.0	6.2
3	0.66**	15.0	28.0	26.0	2.2*
10	1.5*	1.9*	4.3	7.3	1.0*
11	28.0	14.0	30.0	29.0	20.0
13	2.8*	38.0	7.0	60.0	12.0
6	0.043***	1.0*	1.2*	7.1	0.28**
5	0.56 (nM)****	3.2*	0.37**	1.5*	2.0*
12	1.32*	nd	29.2	nd	6.7
8[d]	0.076***	nd	0.19**	nd	0.023***
7	1.07*	nd	21.3	nd	2.1*
14	0.10**	nd	2.98*	nd	1.7*
15	1.58*	nd	13.2	nd	20

[≠]Curcuminoids with: $IC_{50} < 4$ micro-molar are considered active*; $IC_{50} < 1$ micro-molar considered highly active**; IC50 < 0.1 micro-molar considered potent***; IC_{50} values in the nano-molar range are considered highly potent****; compounds were chemically stable at r.t. in DMSO (solvent used for bioassay). nd = not determined.

[a] IC_{50} is drug concentration that can inhibit 50% of cell growth.

[b] Cell viability was analyzed by the CellTiter-Glo® Luminescent Cell Viability Assay.

[c] Cell viability was analyzed by the MTT assay.

[d] Contained circa 25% of the diketo-tautomer **9**.

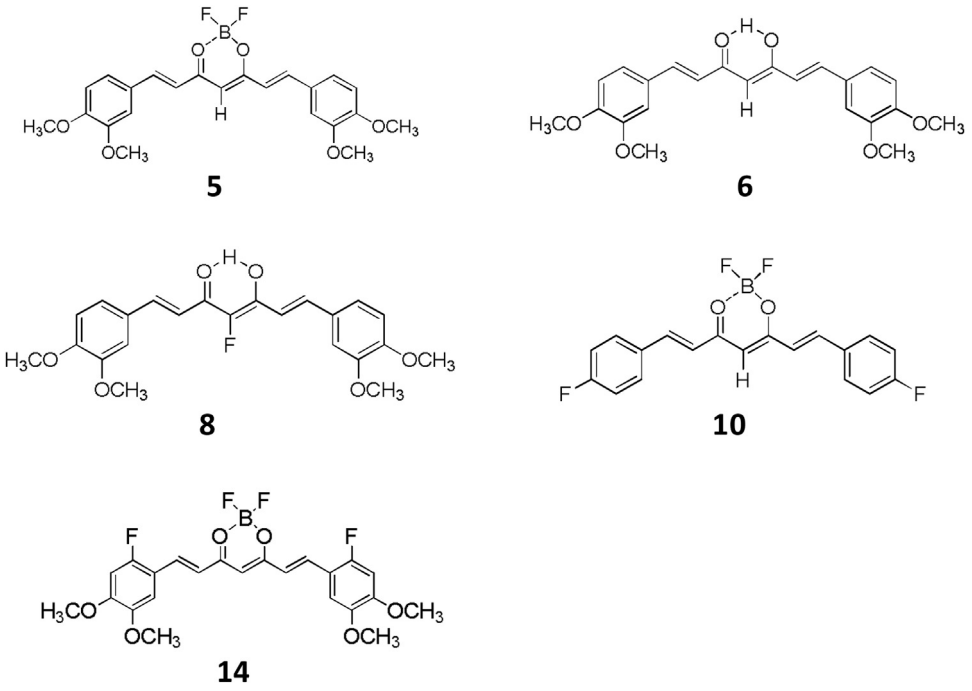

Fig. 9. Most potent curcuminoids identified based on bioassay.

with the bioactivity data (IC_{50} MDA231; breast cancer) in the search for correlations between the HER2 inhibitory activity and inhibition of cancer cells growth.

The curcuminoid derivatives fitted nicely in the tunnel-like binding pocket of HER2, where they mainly established hydrophobic contacts. The more bioactive analogs (as in **14**) interacted with the residues Leu726, Thr798, Lys753, Leu796, Thr862, Asp863, Val734, and Leu852 (Figs. 10 and 11), similar to the potent HER2 tyrosine kinase domain (HER2-TK) inhibitor SYR127063 (2-{2-[4-({5-chloro-6-[3-(trifluoromethyl))phenoxy]pyridin-3-yl}amino)-5H-pyrrolo[3,2-d]pyrimidin-5-yl]ethoxy}ethanol). In addition to its numerous hydrophobic interactions, SYR also formed hydrogen bonds with Met801, Asp863 and Asn850. A hydrogen bond with Met801 was also observed for the difluorinated curcuminoid **3**. Table S2 (Supplementary data) provides a comparison between docking energies in HER2 and the measured IC_{50} values for MDA231, showing that curcuminoids-BF_2 adducts **10**, **14**, and **5** exhibit both favorable docking energy and cytotoxicity against breast cancer. Inhibition of tumor cellular proteasome has been suggested as the mechanism by which curcumin arrests the proliferation of acute promyelocytic leukemia (APL) cells [5]. Considering the high degree of potency against leukemia observed in the present study, in particular by **5**, **6**, **8**, and **14**, docking calculations were also performed in proteasome (Table S3, Supplementary data). The structure of the 20S proteasome (β5 and β6 subunits) was obtained from the Protein Data Bank. Treatment with proteasome inhibitors results in decrease proliferation, induction of apoptosis, and sensitization of a variety of tumor cells to chemotherapeutic agents and irradiation. Docking calculations for curcuminoids resulted in binding energies that were similar to parent curcumin itself, but judging from their IC_{50} values these compounds are more active.

Considering the high bioactivity and favorable docking energies of compounds **5**, **6**, **8**, **10**, and **14**, their electrostatic potential maps were computed and are shown in Fig. 12 for a better visualization of the electronic properties of these molecules. Molecular electrostatic potential is a useful tool for interpreting and getting insight into the role played by electrostatic forces in the interactions between biomolecules and their ligands.

For this family of compounds the most notable observation is the negative electrostatic potential developed by the BF_2 and the keto-enol moiety.

3. Comparative discussion and summary

A series of fluorinated curcumins and curcumin-BF_2 adducts have been synthesized and characterized. The α-carbonyl mono- and difluorinations were achieved by direct fluorination with Selectfluor, and ring fluorinated/trifluoromethylated CUR-BF_2 adducts were assembled in one-pot from the corresponding aldehydes. Structural features of the new curcuminoids were examined by multinuclear NMR, and by X-ray analysis (for three CUR-BF_2 adducts and a mono-fluorinated analog). A notable feature observed in the X-ray crystal structures is detection of intermolecular interactions via short H-F contacts. The IC_{50} data from *in-vitro* cell growth inhibitory bioassay indicated that the majority of curcuminoids were more active relative to parent curcumin, but those shown in Fig. 10 were clearly superior. The bioassay data along with the NCI-60 screening suggest that CUR-BF_2 complexes bearing activating substituents in the phenyl rings (as in **5**) may be promising drug candidates, and that introduction of F or CF_3 groups into the phenyl rings is not particularly beneficial. The finding that **8** is more potent than **6** implies that monofluorinaton at the α-carbonyl position can be beneficial. The fact that activity of F_2-CUR analogs (**3**, **12**, **7**, and **16**) were not particularly impressive reinforces the earlier conclusions that the enolic tautomer is an important feature in binding of curcumin to proteins [1,5]. Model molecular docking calculations in the active site of HER2 indicated that the curcuminoid derivatives can fit nicely in the tunnel-like binding pocket of HER2 by establishing hydrophobic contacts, leading to favorable docking energies. In summary, the present study has provided notable structural clues that when brought to bear could lead to the synthesis of effective drug targets based on curcumin. Synthesis and characterization of

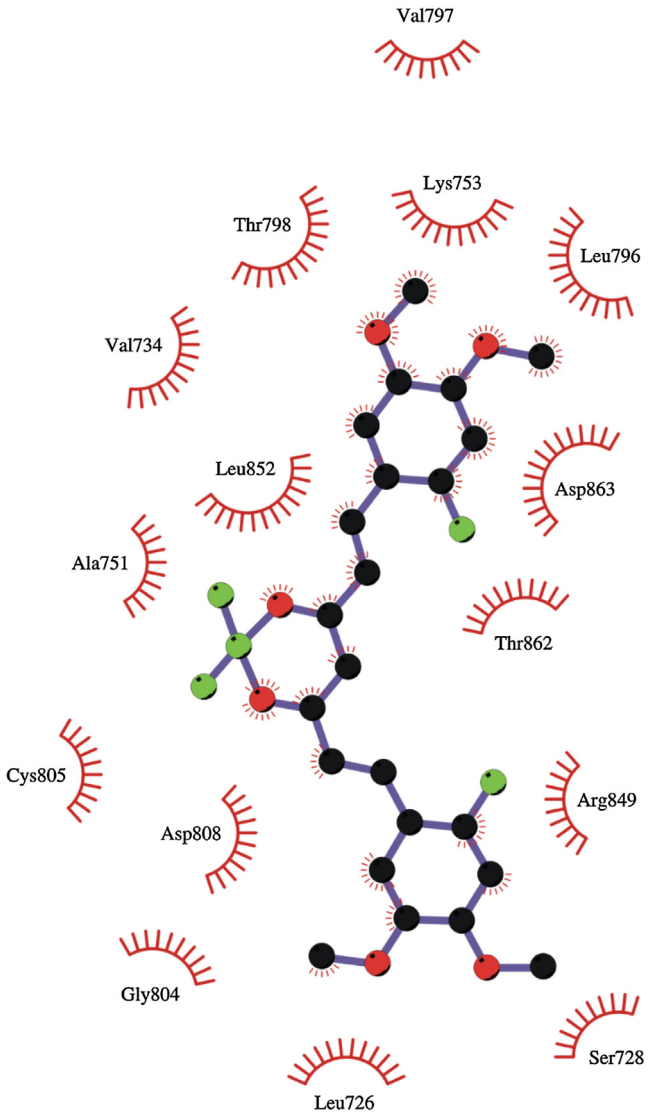

Fig. 10. Binding mode in the active site of HER2 of compound **14** as a model curcuminoid analog (2D-plot).

other fluorocurcuminoids, including those bearing heterocyclic aryl rings, are ongoing in this laboratory and collaborative studies aimed at understanding how fluorination contributes to inhibition of cell viability are planned.

4. Experimental section

4.1. General

Synthetic curcumin, fluorinated aldehydes (*p*-fluorobenzaldehye, 6-fluorovetraldehyde, vetraldehyde, and *p*-trifluoromethylbenzaldehyde), Selectfluor, and acetylacetone were all high purity commercially available samples and were used without further purification. Regular solvents used for synthesis (MeCN, acetone, DCM, hexane, and EtOAc) were all of sufficient purity and were used as received. Column chromatography was performed on silica gel (63–200 mesh). NMR spectra were recorded on a 500 MHz instrument using $CDCl_3$, DMSO-d_6, or MeCN-d_3 as solvent. ^{19}F NMR and ^{11}B NMR spectra were referenced relative to external $CFCl_3$ and $BF_3{\cdot}Et_2O$ respectively. HRMS analyses were performed on an LC–MS instrument in electrospray mode using DMSO as solvent. FT-IR spectra were recorded in ATR mode in solvent. Microwave reactions were performed in a miniature 400 W lab microwave in 5 mL vials with magnetic stirring. Melting points were measured in open capillaries and are not corrected.

4.2. Typical procedure for difluorination of curcuminoids

Selectfluor (2.2 equiv.) was added in one portion to a solution of the curcuminoid (0.75 mmol) in methanol (25 mL) at r.t. (at 55 °C in case of compounds **6** and **11**) with efficient stirring under a nitrogen atmosphere for the requisite time (either 4 h at 55 °C or overnight for r.t.) until completion (TLC monitoring). The MeOH solvent was then removed *in vacuo* and the reaction mass was dissolved in DCM (3 × 10 mL), washed with deionized water (3 × 10 mL), dried (sodium sulfate) and filtered through a coarse sintered glass funnel. The DCM was removed *in vacuo* and the crude mixture was purified by flash chromatography eluting with hexane and ethyl acetate (refer to analytical data), ramping of the elution solvent was employed in all cases.

4.3. Specific procedure – difluorination of 11

Selectfluor (371 mg, 1.04 mmol, 2.5 equiv.) was added in one portion to a solution of **11** (0.42 mmol, 131 mg) in methanol (20 mL) under a nitrogen atmosphere, and the mixture was stirred under mild reflux at 55 °C overnight. Completion of the reaction was confirmed by TLC and the solvent was removed *in vacuo*. The reaction mass was dissolved in DCM (3 × 10 mL) and washed with deionized water (3 × 10 mL). The organic layer was dried (sodium sulfate), filtered through a coarse sintered glass funnel, and the solvent was removed *in vacuo*. The difluoro-derivative (compound **12**) precipitated out of the crude reaction mixture as a white crystalline solid by addition of hexane/EtOAc (20%); 62 mg, 0.18 mmol, 42% yield.

4.4. Typical procedure for monofluorination of curcuminoids

Selectfluor (0.8 mmol, 1.05 equiv.) was added in one portion to a solution of the curcuminoid (0.75 mmol) in acetonitrile (25 mL) at 0 °C under a nitrogen atmosphere, and the mixture was stirred for 6 h at this temperature, followed by overnight stirring at r.t. Upon completion (verified by TLC) the solvent was removed *in vacuo* and the reaction mass was dissolved in DCM (3 × 10 mL). The reaction mixture was washed with deionized water (3 × 10 mL), dried over sodium sulfate and filtered through a coarse sintered glass funnel. The solvent was removed *in vacuo* and the crude reaction mixture was purified by flash chromatography eluting with hexane/ethyl acetate (refer to analytical data), ramping of the elution solvent was employed in all cases).

4.5. Specific procedure – monofluorination of 11

Selectfluor (286 mg, 0.81 mmol, 1.05 equiv.) was added in one portion to a solution of **11** (119 mg, 0.38 mmol) in acetonitrile (20 mL) at 0 °C under a nitrogen atmosphere, and the mixture was stirred for 6 h at this temperature, followed by overnight stirring at r.t. Upon completion (monitored by TLC), the acetonitrile was removed *in vacuo* and the reaction mass was dissolved in DCM (3 × 10 mL). Following the steps outlined in the typical procedure and flash chromatography using hexane/EtOAc (5%), the monofluorinated product **13** was obtained as a yellow solid (54 mg, 0.16 mmol, 43% yield).

4.6. Synthesis of acetylacetone-difluoroboron adduct

Following a similar procedure described by Fraser et al. [29], to a mixture of acetylacetone (10 mmol, 1.00 g) in dry DCM (50 mL,

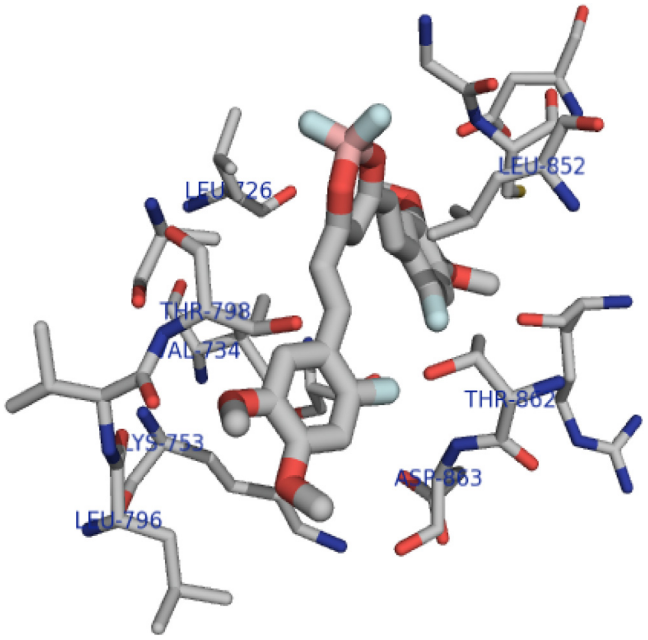

Fig. 11. Binding mode in the active site of HER2 of compound **14** as a model curcuminoid analog (3D-plot).

distilled from P_2O_5) under a nitrogen atmosphere $BF_3{\cdot}Et_2O$ (~48%; 2.13 g, 1.89 mL, 15 mmol, 1.5 equiv.) was slowly added over a period of 5 min, and the reaction mixture was refluxed (41 °C) for 12 h. Upon completion of the reaction, the reaction mixture was allowed to come to room temperature and quenched with DI water (15 mL). It was transferred to a large separatory funnel, the DCM layer was separated, and the aqueous layer was discarded (the aqueous layer was quite acidic with a pH of about 1 or less). The reaction mixture was subsequently washed several times with DI water (3 × 15 mL) until the aqueous layer had a pH of about 7. The organic layer was dried (sodium sulfate), filtered through a coarse sintered glass funnel, and the solvent was removed *in vacuo* to afford a brown crystalline solid (1.42 g, 9.61 mmol, 96.0% yield), which was shown to be pure by NMR.

4.7. Typical procedure for the synthesis of curcuminoid-difluoroboron adducts

These compounds were synthesized by a slight modification of the procedure described by Rao and Sudheer [20]. To a mixture of acetylacetone-BF_2 complex (887 mg, 6 mmol) in ethyl acetate (60 mL) under stirring and nitrogen atmosphere, the respective aldehyde (2.2 equivalence, 13.2 mmol) was added in one portion, followed by N-butylamine (0.22 eq., 1.32 mmol, 96.5 mg, 130 μL) over a period of 20 min, with continuous stirring at room temperature overnight. The completion of the reaction was confirmed by TLC. The desired product precipitates from ethyl acetate. The reaction mixture was cooled to 0 °C in an ice bath and the product was filtered, washed with cold (0 °C) ethyl acetate and dried for 30 min. The purity of this cut was exceptional (NMR) and no further purification was required (~60% isolated yield). The filtrate was transferred to a round bottom flask and concentrated under vacuum and re-filtered to obtain a second cut which was slightly less pure by NMR (combined yield: typically > 80%, except for compound **2** which was 64%).

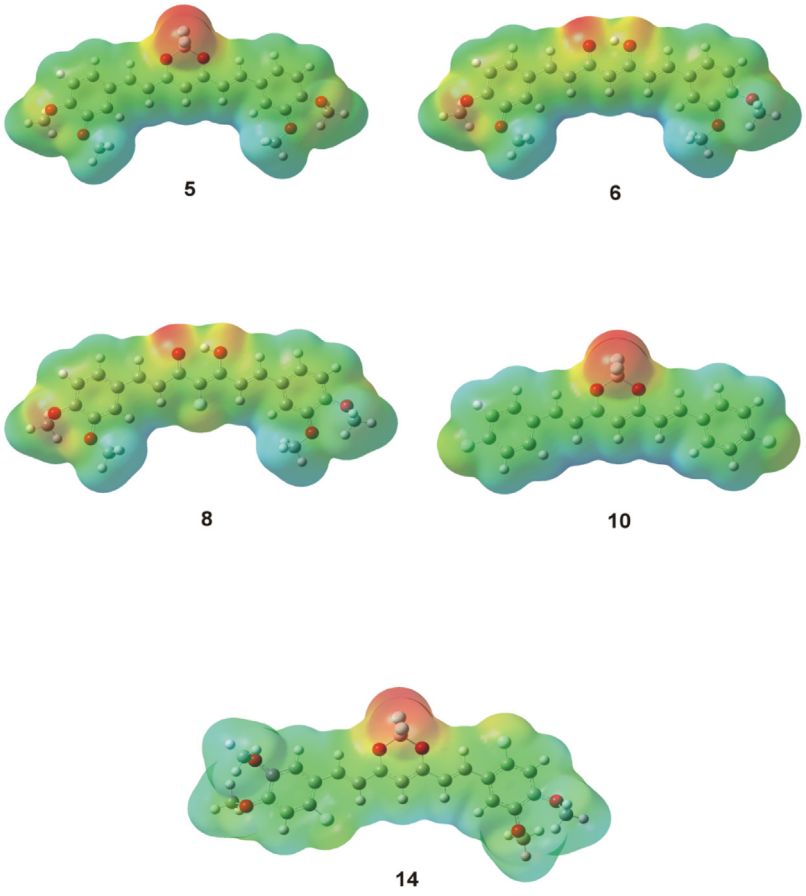

Fig. 12. Electrostatic potential maps for the most active curcuminoid derivatives.

4.8. Specific procedure – synthesis of curcuminoid-BF_2 adduct 10

To a mixture of acetylacetone-BF_2 (887 mg, 6.00 mmol) in ethyl acetate (60 mL) under stirring and nitrogen atmosphere, was added *p*-fluorobenzaldehyde (2.2 equiv., 13.2 mmol, 1.638 g) in one portion, followed by slow addition (over 20 min) of N-butylamine (0.22 equiv., 1.32 mmol, 96.5 mg, 130 μL). The reaction mixture was stirred continuously at room temperature overnight whereupon compound **10** precipitated from ethyl acetate. The reaction mixture was cooled to 0 °C in an ice bath, filtered, and the product was washed with cold (0 °C) ethyl acetate and dried for 30 min to afford compound **11** as a yellow solid (1.72 g, 4.78 mmol, 80% yield) which was confirmed by NMR to be highly pure.

4.9. General procedure for decomplexation of curcuminoid-BF_2

Using a modified microwave assisted method [26], the curcuminoid-BF_2 complex (0.3 mmol) and sodium oxalate (2 equiv) were added to a clean/dry microwave vial equipped with magnetic stirrer. Aqueous methanol (5 mL, 8:2 MeOH/H_2O) was added and the vial was sealed with a crimp-able cap with septa using a crimping tool and the sealed vial was irradiated for 6 min at 140 °C. The vial was cooled to room temperature and the cap removed. The reaction mixture was transferred to a round bottom flask and the methanol removed under vacuum. Upon addition of deionized-water (20 mL) a precipitate was formed which was collected by filtration, washed with 40 mL of deionized-water and dried for 30 min. The resulting curcuminoid product was >98% pure (by NMR).

4.10. Typical procedure – decomplexation of curcuminoid-BF_2 adduct 10

The curcuminoid-BF_2 adduct **10** (101 mg, 0.28 mmol) and sodium oxalate (75 mg, 0.56 mmol, 2 equiv.) were added to a clean/dry microwave vial equipped with magnetic stirrer. Upon addition of aqueous methanol (5 mL, 8:2 MeOH/H_2O) a suspension was formed. The vial was sealed and irradiated for 6 min at 140 °C. The vial was cooled to r.t. and the sealed cap was removed. Removal of solvent and addition of deionized-water gave a precipitate which was washed and dried under vacuum to give compound **11** as a yellow solid (79 mg, 0.25 mmol, 90% yield) which was pure by NMR.

4.11. Microwave assisted formation of curcumin-BF_2 adduct using selectfluor

To a clean dry microwave vial (5 mL) curcumin **1** (276 mg, 0.75 mmol) was added followed by acetone (5 mL) to dissolve the curcumin. Selectfluor (292 mg, 0.82 mmol, 1.1 equiv) was then added directly to the solution, and the vial was sealed with a crimp-able cap with septa using a crimping tool. The absorbance was set to very high and the mixture was irradiated at 200 W for 97 s until it reached a temperature of 138 °C and a pressure of 10 bar. The reaction was monitored by TLC at intervals by removing ~0.1 mL through the septa with a syringe and diluting in DCM. Upon completion, the acetone was removed *in vacuo* and reaction mass was dissolved in DCM, washed with deionized water (3 × 10 mL), dried (sodium sulfate) and filtered through a coarse sinter glass funnel. The solvent was removed *in vacuo*, and the crude mixture was purified by flash chromatography eluting with ethyl acetate/hexane (40:60). The resulting curcumin-BF_2 complex **2** (128 mg, 0.307 mmol, 41% yield) was pure as confirmed by NMR. For comparison, a 64% isolated yield was obtained for this decomplexation by using $BF_3{\cdot}Et_2O$ instead of Selectfluor.

5. Characterization data

*5.1. Curcumin-BF_2 adduct **(2)***

Yield: 64% (using $BF_3{\cdot}Et_2O$) and 41% (by using Selectfluor), red solid, mp > 260 °C. Rf 0.16 (40% EtOAc in hexane). ^{1}H NMR (CD_3CN, 500 MHz): δ 7.96 (d, J = 16.0 Hz, 2H), 7.42 (br s, 2OH), 7.37 (d, J = 2.1 Hz, 2H), 7.30 (dd, J = 8.2 and 2.1 Hz, 2H), 6.94 (d, J = 8.6 Hz, 2H), 6.89 (d, J = 16.0 Hz, 2H), 6.28 (s, 1H), 3.95 (s, 6H, 2OMe). ^{13}C NMR (CD_3CN, 125 MHz): δ 180.5, 151.4, 148.7, 147.6, 127.8, 128.0, 119.2, 116.2, 112.3, 102.4, 56.7.^{19}F NMR (CD_3CN, 470 MHz): δ −140.97 (s, ^{11}B F), −140.91 (s, ^{10}B F). ^{11}B NMR (CD_3CN, 160.3 MHz): δ 0.95 (s).

*5.2. (*1E,6E*)-4,4-Difluoro-1,7-bis(4-hydroxy-3-methoxyphenyl) hepta-1,6-diene-3,5-dione **(3)***

Yield: 33%, red solid, mp 117–118 °C. Rf 0.53 (40% EtOAc in hexane). ^{1}H NMR (CD_3CN, 500 MHz): δ 7.85 (d, J = 16.0 Hz, 2H), 7.35 (d, J = 1.5 Hz, 2H), 7.29 (br s, 2OH), 7.25 (dd, J = 8.0 and 1.5 Hz, 2H), 7.12 (d, J = 16 Hz, 2H), 6.88 (d, J = 8.0 Hz, 2H), 3.90 (s, 6H, 2OMe). ^{13}C NMR (CD_3CN, 125 MHz): δ 186.5 (t, $^2J_{CF}$ 26.7 Hz), 150.5, 148.8, 147.8, 126.2, 125.5, 115.2, 116.5, 111.1, 111.7 (t, $^1J_{CF}$ = 263.2 Hz), 58.9. ^{19}F NMR (CD_3CN, 470 MHz): δ - 115.3. HRMS (ESI): m/z $[M+H]^+$ calcd for $C_{21}H_{19}O_6F_2$: 405.1149; found: 405.065. IR (cm^{-1}, CH_2Cl_2/MeCN): 3415 (br, OH), 3182-2847 (C-H package), 1693 (CO), 1681, 1568, 1506, 1431, 1271, 1207, 1122, 1064.

*5.3. (*1E,4E,6E*)-4-Fluoro-5-hydroxy-1,7-bis(4-hydroxy-3-methoxyphenyl)hepta-1,4,6-trien-3-one **(4)***

Yield: 52%, purple solid, mp 154–155 °C. Rf 0.60 (40% EtOAc in hexane). ^{1}H NMR (CD_3CN, 500 MHz): δ 14.1 (br, enolic OH), 7.63 (d, J = 16 Hz, 2H), 7.31 (d, J = 16 Hz, 2H), 7.20 (dd, J = 8.5 and 1.5 Hz, 2H), 7.10 (dd, J = 16 and 3.5 Hz, 2H), 7.05 (s, 2H, 2OH), 6.87 (d, J = 8.0 Hz, 2H), 3.91 (s, 6H, 2OMe). ^{13}C NMR (CD_3CN, 125 MHz): 172.1 (d, $^2J_{CF}$ = 23 Hz), 149.5, 147.7, 143.0 (d, $^1J_{CF}$ = 238.0 Hz), 141.9 (d, $^3J_{CF}$ = 2.9 Hz), 127.4, 123.8, 115.1, 114.3, 110.7, 55.8. ^{19}F NMR (CD_3CN, 470 MHz): δ - 176.5 (t, J_{HF} = 2.8 Hz). HRMS (ESI): m/z $[M+H]^+$ calcd for $C_{21}H_{20}O_6F$: 387.1243; found: 387.080. IR (cm^{-1}, CH_2Cl_2/MeCN): 3417 (br, OH), 3062-2937 (C-H package), 1620 (CO), 1568, 1504, 1429. 1267, 1122, 1029.

*5.4. Tetramethoxy-curcuminoid-BF_2 complex **(5)***

Yield 83%, purple solid, mp 224–226 °C, Rf 0.16 (40% EtOAc in hexane). ^{1}H NMR (DMSO-d_6, 500 MHz): δ 7.97 (d, J = 16.0 Hz, 2H), 7.49 (d, J = 2.0 Hz, 2H), 7.46 (dd, J = 8.0 and 2.0 Hz, 2H), 7.11 (d, J = 16 Hz, 2H), 7.07 (d, J = 8.0 Hz, 2H), 6.50 (s, 2H), 3.84 (s, 6H). ^{13}C NMR (DMSO-d_6, 125 MHz): δ 179.5, 153.0, 149.6, 147.3, 127.6, 125.6, 119.3, 112.3, 111.7, 101.8, 56.3, 56.1.^{19}F NMR (DMSO-d_6, 470 MHz): δ - 137.9 (s, ^{11}B F), −137.8 (s, ^{10}B F). ^{11}B NMR (DMSO-d_6, 160.3 MHz): δ 0.90 (s). IR (cm^{-1}, CH_2Cl_2): 3003-2841 (CH package), 1610 (CO), 1529, 1508, 1263, 1136.

*5.5. (*1E,4E,6E*)-5-Hydroxy-1,7-bis(3,4-dimethoxyphenyl)hepta-1,4,6-trien-3-one (6)*

Yield 94%, red solid, mp 122–125 °C. Rf 0.37 (40% EtOAc in hexane). ^{1}H NMR ($CDCl_3$, 500 MHz): δ ~14.8 (br, enolic OH),7.62 (d, J = 16.0 Hz, 2H), 7.17 (dd, J = 8.0 and 1.6 Hz, 2H), 7.09 (d, J = 1.5 Hz, 2H), 6.89 (d, J = 8 Hz, 2H), 6.51 (d, J = 16 Hz, 2H), 5.85 (s, 1H), 3.94 (s, 6H), 3.93 (s, 6H). ^{13}C NMR (DMSO-d_6, 125 MHz): δ 183.6, 151.4, 149.5, 140.9, 128.0, 123.5, 122.5, 112.1, 110.8, 101.5, 56.0, 56.1. HRMS (ESI): m/z $[M+H]^+$ calcd for $C_{23}H_{25}O_6$: 397.1651; found: 397.140. IR (cm^{-1}, DCM/CH_2Cl_2): 3005-2837 (CH package), 1624 (CO), 1581, 1510, 1462, 1259, 1136, 1022.

*5.6. (*1E,6E*)-4,4-Difluoro-1,7-bis(3,4-dimethoxyphenyl)hepta-1,6-diene-3,5-dione* ***(7)***

Yield: 40%, orange solid, mp 148–149 °C. Rf 0.42 (40% EtOAc in hexane). ^{1}H NMR ($CDCl_3$, 500 MHz): δ 7.87 (d, J = 15.5 Hz, 2H), 7.24 (dd, J = 8.0 and 2.0 Hz, 2H), 7.13 (d, J = 2.0 Hz, 2H), 6.98 (d, J = 15.5 Hz, 2H), 6.90 (d, J = 8.0 Hz, 2H), 3.95 (s, 6H, 2OMe), 3.96 (s, 6H, 2OMe). ^{13}C NMR ($CDCl_3$, 125 MHz): δ 186.6 (t, $^2J_{CF}$ 26.8 Hz), 152.7, 149.4, 148.8, 126.7, 125.1, 115.6, 112.0 (t, $^1J_{CF}$ = 264.1 Hz), 111.0, 110.0, 59.0. ^{19}F NMR ($CDCl_3$, 470 MHz): δ - 115.3 (s, ^{11}B isotope) and −115.4 (s, ^{10}B isotope). HRMS (ESI): *m/z* $[M+H]^+$ calcd for $C_{23}H_{23}O_6F_2$: 433.1462; found: 433.0886. IR (cm^{-1}, CH_2Cl_2/DCM): 3003-2937 (CH package), 1681(CO), 1587, 1573, 1510, 1463, 1421, 1265, 1139.

*5.7. (*1E,4E,6E*)-4-Fluoro-5-hydroxy-1,7-bis(3,4-dimethoxyphenyl) hepta-1,4,6-trien-3-one (8) and (1E,6E)-4-Fluoro-1,7-bis(3,4-dimethoxyphenyl)hepta-1,6-diene-3,5-dione (9)*

Tautomeric mixture (75:25 ratio by ^{19}F NMR). Yield 33%, red solid, mp 145–146 °C. Rf 0.52 (40% EtOAc in hexane). Analytical data for **8**. ^{1}H NMR ($CDCl_3$, 500 MHz): δ ~14.0 (br, enolic OH), 7.67 (d, J = 16 Hz, 2H), 7.21 (dd, J = 8.0 and 2.0 Hz, 2H), 7.14 (d, J = 2 Hz, 2H), 6.99 (dd, J = 16.0 and 3.5 Hz, 2H), 6.90 (d, J = 8.5 Hz, 2H), 3.96 (s, OMe), 3.94 (s, OMe).^{19}F NMR ($CDCl_3$, 470 MHz): δ - 175.7 (s). Analytical data for **9**: ^{1}H NMR ($CDCl_3$, 500 MHz): δ 7.78 (d, J = 16 Hz, 2H), 7.22 (dd, not fully resolved), 7.12 (d, J = 2 Hz), 6.88 (d, J = 8.5 Hz), 5.70 (d, J_{HF} = 50 Hz), 3.93 (s, OMe), 3.94 (OMe, not fully resolved). ^{19}F NMR ($CDCl_3$, 470 MHz): δ − 194.9 (d, J_{HF} = 50 Hz). Data for **8** (a) and **9** (b): ^{13}C NMR ($CDCl_3$, 125 MHz): 189.9 (d, $^2J_{CF}$ = 20 Hz)^b, 172.0 (d, $^2J_{CF}$ = 22 Hz)^a, 152.3, 151.4^a, 149.3, 149.2^a, 146.9 (d, $^3J_{CF}$ = 2.7 Hz)^b, 143.0 (d, $^1J_{CF}$ = 236 Hz)^a, 141.7 (d, $^3J_{CF}$ = 3 Hz)^a, 128.0^a, 126.9^b, 123.2^a, 117.1^b, 115.0^a, 111.1^a, 111.0, 109.9^a, 97.5 (d, $^1J_{CF}$ = 199 Hz)^b, 56.0, 55.0. HRMS (ESI): *m/z* $[M+H]^+$ calcd for $C_{23}H_{24}O_6F$: 415.1556; found: 415.120. IR (tautomeric mixture; cm^{-1}, CH_2Cl_2/$CDCl_3$): 3400 (br, OH), 2933, 2839, 1685 (CO), 1589, 1510, 1463, 1265, 1139, 1022.

5.8. Difluorocurcuminoid-BF_2 adduct ***(10)***

Yield 80%, orange solid, mp 258–260 °C. Rf 0.05 (5% EtOAc in hexane). ^{1}H NMR (acetone-d_6, 500 MHz): δ 8.07 (d, J = 15.7 Hz, 2H), 7.96 (dd, J = 8.5 and 7.0 Hz, 4H), 7.30 (t appearance, J = 9.5 Hz, 4H), 7.13 (d, J = 15.7 Hz, 2H), 6.65 (s, 1H). ^{13}C NMR (acetone-d_6, 125 MHz): δ 181.7, 165.7 (d, $^1J_{CF}$ = 251.7 Hz), 146.3, 132.7 (d, J_{CF} = 8.6 Hz), 131.9 (d, JCF = 3.9 Hz), 122.2, 117.2 (d, J_{CF} = 22 Hz), 103.1.^{19}F NMR (acetone-d_6, 470 MHz): δ - 108.7 (m, 2F), −140.2 (s, ^{11}B F), −140.1 (s, ^{10}B F).^{11}B NMR (acetone-d_6, 160.3 MHz): δ 1·01 (s). IR (cm^{-1}, CH_2Cl_2): 3107, 3041, 2922, 2850, 1620 (CO), 1589, 1548, 1508, 1404, 1232, 1155.

*5.9. (*1E,4E,6E*)-1,7-Bis(fluorophenyl)-5-hydroxy-hepta-1,4,6-trien-3-one* ***(11)***

Yield 90%, yellow solid, mp 158–160 °C, Rf 0.32 (5% EtOAc in hexane). ^{1}H NMR ($CDCl_3$, 500 MHz): δ ~15.9 (br, enolic OH), 7.64 (d, J = 16.0 Hz, 2H), 7.56 (dd, J = 8.5 and 15.0 Hz, 4H), 7.10 (t appearance, J = 8.5 Hz, 4H), 6.51 (d, J = 15.9 Hz, 2H), 5.82 (s, 1H). ^{13}C NMR ($CDCl_3$, 125 MHz): δ 183.1, 163.8 (d, $^1J_{CF}$ = 250.8 Hz), 139.4, 131.2 (d, J_{CF} = 2.9 Hz), 129.9 (d, J_{CF} = 8.6 Hz), 123.7, 116.1 (d, J_{CF} = 22 Hz), 101.8. ^{19}F NMR ($CDCl_3$, 470 MHz): δ - 109.7 (m). HRMS (ESI): *m/z* $[M+H]^+$ calcd for $C_{19}H_{15}O_2F_2$: 313.1040; found: 3313.100. IR (cm^{-1}, DCM): 3066-2850 (CH package), 1631 (CO), 1593, 1508, 1414, 1234, 1150.

*5.10. (*1E,6E*)-4,4-Difluoro-1,7-bis(4-fluorophenyl)hepta-1,6-diene-3,5-dione* ***(12)***

Yield 42%, white solid, mp 72–73 °C, Rf 0.35 (5% EtOAc in hexane). ^{1}H NMR ($CDCl_3$, 500 MHz): δ 7.88 (d, J = 16.5 Hz, 2H), 7.67–7.63 (m, 4H), 7.15–7.12 (m, 4H), 7.06 (d, J = 16.5 Hz, 2H). ^{13}C NMR ($CDCl_3$, 125 MHz): δ 186.7 (t, $^2J_{CF}$ 27.9 Hz), 164.9 (d, $^1J_{CF}$ = 254.7 Hz), 147.3, 131.4 (d, J_{CF} = 8.5 Hz), 129.9 (d, J_{CF} = 3.9 Hz), 117.6 (d, J_{CF} = 2.9 Hz), 116.4 (d, J_{CF} = 22 Hz), 111.4 (t, $^1J_{CF}$ = 265.1 Hz). ^{19}F NMR ($CDCl_3$, 470 MHz): δ - 106.2 (m, 2F), −115.3 (s, 2F). HRMS (ESI): *m/z* $[M+H]^+$ calcd for $C_{19}H_{13}O_2F_4$: 349.0851; found: 349.040. IR (cm^{-1}, DCM/$CDCl_3$): 3078, 2929, 1697, 1608, 1585, 1508, 1417, 1234, 1159, 1112, 1099, 1058.

*5.11. (*1E,4E,6E*)-4-Fluoro-1,7-bis(4-fluorophenyl)-5-hydroxy-hepta-1,4,6-trien-3-one* ***(13)***

Yield: 43%, yellow solid, mp 152–153 °C. Rf 0.45 (5% EtOAc in hexane). ^{1}H NMR ($CDCl_3$, 500 MHz): δ ~13.8 (br, enolic OH), 7.68 (d, J = 15.9 Hz, 2H), 7.62 (dd, J = 8.5 and 5.5. Hz, 4H), 7.12 (t appearance, J = 8.5, 4H), 7.06 (dd, J = 15.7 and 3.7 Hz, 2H). ^{13}C NMR ($CDCl_3$, 125 MHz): 172.0 (d, $^2J_{CF}$ = 21.8 Hz), 164.0 (d, $^1J_{CF}$ = 251.6 Hz), 145.5, 143.1 (d, $^1J_{CF}$ = 238.4 Hz), 140.6 (d, J_{CF} = 1.9 Hz), 131.2 (d, J_{CF} = 2.9 Hz, 130.3 (d, J_{CF} = 8.7 Hz), 116.8, 116.2 (d, J_{CF} = 22.0 Hz). ^{19}F NMR ($CDCl_3$, 470 MHz): δ - 108.9 (m, 2F), −175.2 (t, J = 3.3 Hz, 1F). HRMS (ESI): *m/z* $[M+H]^+$ calcd for $C_{19}H_{14}O_2F_3$: 331.0945; found: 331.110. IR (cm^{-1}, DCM/$CDCl_3$): 3072, 2920, 1633, 1597, 1508, 1417, 1319, 1232, 1157.

5.12. Tetramethoxydifluoro-curcuminoid-BF_2 adduct (14)

Yield 90%, red solid, mp 253–255. Rf 0.21 (40% EtOAc in hexane). ^{1}H NMR (DMSO-d_6, 500 MHz): δ 8.05 (d, J = 16.0 Hz, 2H), 7.46 (d, J = 7.0 Hz, 2H), 7.16 (d, J = 15.5 Hz, 2H), 7.08 (d, J = 12 Hz, 2H), 6.65 (s, 1H). ^{13}C NMR (DMSO-d_6, 125 MHz): δ 179.3, 157.2 (d, $^1J_{CF}$ = 250 Hz), 153.9 (d, J_{CF} = 11.4 Hz), 145.9, 138.3 (d, J_{CF} = 2.9 Hz), 120.7 (d, J_{CF} = 5.7 Hz), 113.1 (d, J_{CF} = 11.4 Hz), 110.4 (d, J_{CF} = 3.8 Hz), 101.7, 100.7 (d, J_{CF} = 28.6 Hz), 56.5, 56.2. ^{19}F NMR (DMSO-d_6, 470 MHz): δ - 119.0 (unresolved dd, 2F), −137.7 (s, ^{11}B F), −137.6 (s, ^{10}B F).^{11}B NMR (DMSO-d_6, 160.3 MHz): δ 0.89 (br s).

IR (cm^{-1}, CH_2Cl_2): 2954, 2922, 2852, 1714, 1597, 1514, 1462, 1278, 1193, 1001.

*5.13. (*1E,4E,6E*)-5-Hydroxy-1,7-bis(3,4-dimethoxy-6-fluorophenyl) hepta-1,4,6-trien-3-one (*15)

Yield 94%, orange solid, mp 154–156 °C. Rf 0.45 (40% EtOAc in hexane). ^{1}H NMR ($CDCl_3$, 500 MHz): δ 7.74 (d, J = 16.0 Hz, 2H), 6.99 (d, J_{HF} = 7.5 Hz, 2H), 6.67 (d, J_{HF} = 12.5 Hz, 2H), 6.60 (d, J = 16.5 Hz, 2H), 5.88 (s, 1H), 3.92 (s, 12H). ^{13}C NMR ($CDCl_3$, 125 MHz): δ 183.2, 156.6 (d, $^1J_{CF}$ = 249.0 Hz), 151.8 (d, J_{CF} = 10.4 Hz), 145.6 (d, J_{CF} = 2.0 Hz), 133.0, 124.0 (d, J_{CF} = 6.6 Hz), 114.1 (d, J_{CF} = 13.3 Hz), 109.6 (d, J_{CF} = 4.8 Hz), 101.4, 100.2 (d, J_{CF} = 28.5 Hz), 56.4, 56.3. ^{19}F NMR ($CDCl_3$, 470 MHz): δ - 120.1 (dd, J_{HF} = 11.7 and 5.6 Hz). HRMS (ESI): *m/z* $[M+H]^+$ calcd for $C_{23}H_{23}O_6F_2$: 433.1462; found: 433.142. IR (cm^{-1}, DCM/CH_2Cl_2): 3005-2835 (CH package), 1614 (CO), 1510, 1440, 1363, 1292, 1273, 1211, 1192, 1139, 1109.

*5.14. (*1E,6E*)-4,4-Difluoro-1,7-bis(3,4-dimethoxy-6-fluorophenyl) hepta-1,6-diene-3,5-dione* ***(16)***

Yield: 26%, brown solid, mp 162–163 °C. Rf 0.53 (40% EtOAc in hexane). ^{1}H NMR ($CDCl_3$, 500 MHz): δ 8.05 (d, J = 16.0 Hz, 2H), 7.05 (d, J = 16.0 Hz, 2H), 7.02 (d, J_{HF} = 6.7 Hz, 2H), 6.67 (d, J_{HF} = 11.6 Hz, 2H), 3.93 (s, 6H, OMe), 3.92 (s, 6H, OMe). ^{13}C NMR ($CDCl_3$, 125 MHz): δ 186.7 (t, $^2J_{CF}$ = 27.6 Hz), 158.0 (d, $^1J_{CF}$ = 252.6 Hz), 153.8 (d, J_{CF} = 10.5 Hz), 145.8 (d, J_{CF} = 2.0 Hz), 140.9, 117.0 (d, J_{CF} = 6.6 Hz), 113.1 (d, J_{CF} = 12.4 Hz), 111.7 (t, $^1J_{CF}$ = 264.2 Hz, CF_2), 109.3 (d, J_{CF} = 3.8 Hz), 100.1 (d, J_{CF} = 28.6 Hz), 56.5, 56.4. ^{19}F NMR ($CDCl_3$, 470 MHz): δ - 115.4 (s, 2F), −117.6 (dd, J_{HF} = 11.7 and 5.8 Hz, 2F). HRMS (ESI): *m/z* $[M+H]^+$ calcd for $C_{23}H_{21}O_6F_4$: 469.1274; found:

469.0499. IR (cm^{-1}, $CDCl_3$/DCM): 308, 2941, 1707, 1693, 1512, 1442, 1365, 1280, 1193.

*5.15. (*1E,4E,6E*)-4-Fluoro-5-hydroxy-1,7-bis(3,4-dimethoxy-6-fluorophenyl)hepta-1,4,6-trien-3-one* ***(17)***

Yield 10%, red solid, mp 148–150 °C. Rf 0.58 (40% EtOAc in hexane). ^{1}H NMR ($CDCl_3$, 500 MHz): δ 7.82 (d, J = 16 Hz, 2H), 7.08–7.03 (m, 4H), 6.67 (d, J_{HF} = 11.5 Hz), 3.93 (s, OMe), 3.942(s, OMe).^{13}C NMR ($CDCl_3$, 125 MHz): 172.0 (d, $^2J_{CF}$ = 21 Hz), 156.9 (d, $^1J_{CF}$ = 250 Hz), 152.2 (d, J_{CF} = 10.4 Hz), 145.7, 143.1 (d, J_{CF} = 238.5 Hz), 134.2, 116.8 (d, J_{CF} = 5.8 Hz), 114.2 (d, J_{CF} = 12.4 Hz), 109.6 (d, J_{CF} = 3.7 Hz), 100.3, 56.4. 56.3. ^{19}F NMR ($CDCl_3$, 470 MHz): δ − 119.5 (dd, J_{HF} = 11.7 and 6.6. Hz, 2F), −175.3 (distorted t, J = 3.3 Hz, 1F). HRMS (ESI): *m/z* $[M+H]^+$ calcd for $C_{23}H_{22}O_6F_3$ 450.1368; found: 451.0632. IR (cm^{-1}, CH_2Cl_2/$CDCl_3$): 2922, 1608, 1548, 1504, 1367, 1276, 1213, 1157, 1066.

*5.16. (*1E,6E*)-4-Fluoro-1,7-bis(3,4-dimethoxy-6-fluorophenyl)hepta-1,6-diene-3,5-dione* ***(18)***

Yield 12% (by NMR). ^{119}F NMR ($CDCl_3$, 470 MHz): δ −195.2 (d, J_{HF} = 50 Hz, 1F), −118.59 (m, 2F)

5.17. Bis-trifluoromethylcurcuminoid-BF_2 adduct ***(19)***

Yield 88%, yellow solid, mp > 260 °C. Rf 0.14 (10% EtOAc in hexane). ^{1}H NMR (DMSO-d_6, 500 MHz): δ 8.14 (d, J = 15.8 Hz, 2H), 8.10 (d, J = 8.5 Hz, 4H), 7.87 (d, J = 8.0 Hz, 4H), 7.44 (d, J = 15.8 Hz, 2H), 6.77 (s, 1H). ^{13}C NMR (DMSO-d_6, 125 MHz): δ 180.6, 145.2, 145.1, 137.7, 131.0 (q, J_{CF} = 31.4 Hz), 130.1, 125.9 (q, J_{CF} = 3.8 Hz), 124.1, 123.9 (q, $^1J_{CF}$ = 272.7 Hz, CF_3), 103.3. ^{19}F NMR (DMSO-d_6, 470 MHz): δ − 61.4 (s, CF_3), −136.5 (^{11}B-F), −136.4 (^{10}B-F). ^{11}B NMR (DMSO-d_6, 160.3 MHz): δ 0·96 (br,s). IR (cm^{-1}, DCM): 1620, 1529, 1514, 1404, 1321, 1166, 1111, 1064.

*5.18. (*1E,4E,6E*)-1,7-Bis(4-trifluoromethyl-phenyl)-5-hydroxy-hepta-1,4,6-trien-3-one* ***(20)***

Yield 88%, yellow solid, mp 153–154 °C, Rf 0.56 (10% EtOAc in hexane). ^{1}H NMR ($CDCl_3$, 500 MHz): δ ~15.9 (br, enolic OH), 7.95 (d, *J* = 8.0 Hz, 2H), 7.79 (d, J = 8.0 Hz, 2H), 7.72 (d, *J* = 15.9 Hz, 2H), 7.13 (d, J = 15.8 Hz, 2H), 6.28 (s, 1H). ^{13}C NMR ($CDCl_3$, 125 MHz): δ 182.9, 138.3, 131.5 (q, J_{CF} = 31.5 Hz), 128.9, 126.9, 125.7 (q, J_{CF} = 4 Hz), 124.0 (q, $^1J_{CF}$ = 271.8 Hz, CF_3), 102.6.^{19}F NMR ($CDCl_3$, 470 MHz): δ - 61.2 (s, CF_3). HRMS (ESI): *m/z* $[M+H]^+$ calcd for $C_{21}H_{15}O_2F_6$: 413.0976; found: 413.087. IR (cm^{-1}, DCM): 2928, 1635 (CO), 1579, 1413, 1330, 1265, 11681128, 1066.

*5.19. (*1E,6E*)-4,4-Difluoro-1,7-bis(4-trifluoromethyl-phenyl)hepta-1,6-diene-3,5-dione* ***(21)***

Yield 36%, white solid, mp 75–76 °C, Rf 0.72 (10% EtOAc in hexane). ^{1}H NMR ($CDCl_3$, 500 MHz): δ 7.93 (d, J = 15.9 Hz, 2H), 7.76 (d, *J* = 8.5 Hz, 4H), 7.71 (d, d, J = 8.5 Hz, 4H), 7.19 (d, J = 16 Hz, 2H). ^{13}C NMR ($CDCl_3$, 125 MHz): δ 186.6 (t, $^2J_{CF}$ = 27.7 Hz), 146.6, 136.8, 133.2 (q, J_{CF} = 3.8 Hz), 129.3, 126.1 (q, J_{CF} = 3.8 Hz), 123.6 (q, $^1J_{CF}$ = 272.7 Hz, CF_3), 120.0, 112.1 (t, ^1J = 265.1 Hz, CF_2).^{19}F NMR ($CDCl_3$, 470 MHz): δ - 63.1 (s, 6F, CF_3), −115.1 (s, 2F, CF_2). HRMS (ESI): *m/z* $[M+H]^+$ calcd for $C_{21}H_{13}O_2F_8$: 449.0787; found: 449.0145. IR (cm^{-1}, $CDCl_3$): 3080, 2933, 1699 (CO), 1608, 1577, 1417, 1319, 1168, 1124, 1066.

*5.20. (*1E,4E,6E*)-4-Fluoro-1,7-bis(4-trifluoromethyl-phenyl)-5-hydroxy-hepta-1,4,6-trien-3-one* ***(22)***

Yield 60% [crude yield, contained **20** (22%) and **19** (18%); 16% yield after recrystallization (purity by NMR was 70%, contained **19** (30%)], orange solid, mp 144–146 °C. Rf 0.64 (10% EtOAc in hexane). ^{1}H NMR ($CDCl_3$, 500 MHz): δ ~13.5 (br, enolic OH), 7.22 (dd, *J* = 15.5 and 3.7 Hz, 2H), 7.76-7-67 (unresolved-m, 10H). ^{19}F NMR ($CDCl_3$, 470 MHz): δ − 62.8 (6F, CF_3), −173.9 (t, J_{HF} = 3.2 Hz, 1F). HRMS (ESI): *m/z* $[M+H]^+$ calcd for $C_{21}H_{14}O_2F_7$: 431.0882; found: 431.0804.

6. Bioassay methods

The cell viability/anti-proliferative activity of the curcuminoids against PC3 (human androgen-insensitive prostate cancer cell line), LNCap (human-androgen sensitive prostate cancer cell line), A549 (lung cancer), and MDA231 (breast cancer) were determined by means of 3-(4,5-dimethyl-2-thiazolyl)-2,5-diphenyl-2H-tetrazolium bromide (MTT) assay (the tetrazolium salt was a commercial sample) [30]. The ability of the curcuminoids to affect proliferations of suspension cell lines (MOLT-4) was tested by the CellTiter-Glo® Luminescent Cell Viability Assay (purchased from Promega Madison, WI, USA) to determine the number of viable cells in culture based on quantitation of the ATP present. The IC_{50} values were obtained from fitting data with GraphPad software to determine the growth inhibition in the presence of test compounds [30].

7. X-ray crystallography

Suitable single crystals for X-ray diffraction studies were obtained for compounds **10, 5** and **8** from ethyl acetate and for **14** from dichloromethane. Crystal data of the compounds were collected by exactly the same method by mounting a crystal onto a thin glass fiber from a pool of Fluorolube™ and immediately placing it under a liquid N_2 cooled stream, on a Bruker AXS diffractometer upgraded with an APEX II CCD detector. The radiation used is graphite monochromatized Mo Kα radiation (λ = 0.7107 Å). The lattice parameters are optimized from a least-squares calculation on carefully centered reflections. Lattice determination, data collection, structure refinement, scaling, and data reduction were carried out using APEX2 Version 2014.11 software package [31,32]. The data were corrected for absorption using the SCALE program within the APEX2 software package [31,32]. The structure were solved using SHELXT [33]. This procedure yielded a number of the C, B, F and O atoms. Subsequent Fourier synthesis yielded the remaining atom positions. The hydrogen atoms are fixed in positions of ideal geometry (riding model) and refined within the XSHELL software package [34]. These idealized hydrogen atoms had their isotropic temperature factors fixed at 1.2 or 1.5 times the equivalent isotropic U of the C atoms to which they were bonded. A few hydrogen atoms could not be adequately predicted via the riding model within the XSHELL software [34], these hydrogen atoms were located via difference-Fourier mapping and subsequently refined. The final refinement of each compound included anisotropic thermal parameters on all non-hydrogen atoms. The crystal data for the compounds are given in Table 1. Packing diagrams [35] and thermal ellipsoid plots along with selected interatomic distances and bond angles are included in Supplementary data.

8. Computational methods

Geometry optimizations of the curcumin derivatives were performed at the B3LYP /6-311 + G(d,p) level [36] with the Gaussian 09 package [37]. Distribution of the electrostatic potential derived from the electron density was estimated by energy calculations at the optimized structures. The programs AutoDock 4.2 [38] and AutoDock Vina [39] were employed to carry out automated molecular docking for estimating the interaction energy and modeling the binding modes between the curcuminoid

ligands and the enzymes HER2 and proteasome. The three-dimensional coordinates of the proteins were obtained from the Protein Data Bank (PDB codes 3PP0 [40] (HER2) and 3SDK [41] (20S proteasome)). Chain A of HER2, and chains K (β5 subunit) and L (β6 subunit) of 20S proteasome were selected as target templates for the docking calculations. Co-crystalized ligands and crystallographic water molecules were removed. Addition of hydrogens, merger of non-polar hydrogens to the atom to which they were linked, and assignment of partial charges were achieved with AutoDockTools. Merz-Kollman partial atomic charges were employed for proteins, and Gasteiger charges were assigned to ligands. The docking area was defined using the AutoDock module AutoGrid. The docking area, defined using the AutoDock module AutoGrid, was constrained to a $30 \times 26.2 \times 30$ Å box centered at the active site, providing proper space for rotational and translational movement of the ligands. With AutoDock 4.2, the Lamarckian genetic algorithm (LGA) was used, default parameters were applied, and the maximum number of energy evaluations was set to 1.0×10^7. For each of the 100 independent runs performed for each ligand a maximum number of 2.7×10^4 genetic algorithm operations were generated on a single population of 150 individuals. Operator weights for crossover, mutation, and elitism were default parameters, 0.80, 0.02, and 1, respectively. The default parameters were used for Vina.

Acknowledgements

B.R. and K.L. thank The Camille and Henry Dreyfus Foundation for summer research support (to B. R.) in the context of a Jean Dreyfus Boissevain Lectureship award to UNF. This research was supported in part by a grant from the University of North Florida's John A. Delaney Presidential Professorship (to K.L.) and by grants from Consejo Nacional de Investigaciones Científicas y Técnicas (CONICET) and the Secretaría de Ciencia y Tecnología de la Universidad Nacional de Córdoba (Secyt-UNC) (to G.B.). We thank Vivian S. Hogan (Kent State) for assistance with crystallization, University of Florida for access to computational facilities at UF High-Performance Computing Center, and NCI of NIH developmental therapeutics program (DTP) for NCI 60 screening.

Appendix A. Supplementary data

Supplementary data associated with this article can be found, in the online version, at http://dx.doi.org/10.1016/j.jfluchem.2016.09.009.

References

[1] S.C. Gupta, S. Prasad, J.H. Kim, S. Patchva, L.J. Webb, I.K. Priyadarsini, B.B. Aggarwal, Nat. Prod. Rep. 28 (2011) 1937–1955 (Review).
[2] A. Vyas, P. Dandawate, P.S. Padhye, A. Ahmad, A.F. Sarkar, Curr. Pharm. Des. 19 (2013) 2047–2069 (Review).
[3] M. Mimeault, S.K. Batra, Chin. Med. 6 (2011) 1–19 (Review).
[4] D. Simoni, M. Rizzi, R. Rondanin, R. Baruchello, P. Marchetti, F.P. Invidiata, M. Labbozzetta, P. Poma, V. Carina, M. Notarbartolo, A. Alaimo, N. D'Alessandro, Biorg. Med. Chem. Lett. 18 (2008) 845–849.
[5] K.-L. Tan, S.-B. Koh, R.P.-L. Ee, M. Khan, M.-L. Go, ChemMedChem 7 (2012) 1567–1579.
[6] C.L. Nieto, M.P. Cabildo, M.P. Cornago, D. Sanz, R.M. Claramunt, M.C. Torralba, M.R. Torres, J. Elguero, J.A. Garcia, A. Lopez, D. Acuna-Castroviejo, Molecules 20 (2015) 15643–15665.
[7] M.W. Amolins, L.B. Peterson, B.S.J. Blagg, Bioorg. Med. Chem. 17 (2009) 360–367.
[8] M. Labbozzetta, R. Baruchello, P. Marchetti, M. Gueli, P. Poma, M. Notarbartolo, D. Simoni, N. D'Alessandro, Chem. Biol. Interact. 181 (2009) 29–36.
[9] R. Narlawar, M. Pickhardt, S. Leuchtenberger, K. Bauman, S. Krause, T. Dyrks, S. Weggen, E. Mandelkow, B. Schmidt, ChemMedChem 3 (2008) 165–172.
[10] S.B. Wan, H. Yang, Z. Zhou, Q.-C. Cui, D. Chen, J. Kanwar, I. Mohammad, Q.P. Dou, T.H. Chan, Int. J. Mol. Med. 26 (2010) 447–455.
[11] L. Feng, Z.F. Song, H.J. Li, Q.-Y. Huai, Chem. Pharm. Bull. 63 (2015) 873–881.
[12] W. Wichitnithd, U. Nimmannit, S. Wacharasindhu, P. Rojsitthisak, Molecules 16 (2011) 1888–1900.
[13] Z. Cheikh-Ali, J. Caron, S. Cojean, C. Bories, P. Couveur, P.M. Loiseau, D. Desmaele, E. Poupon, P. Champy, ChemMedChem 10 (2015) 411–418.
[14] R. Sribalan, M. Kirubavathi, G. Banuppriya, V. Padmini, Bioorg. Med. Chem. Lett. 25 (2015) 4282–4286.
[15] K. Wada, J.Y. Lee, H.Y. Hung, Q. Shi, L. Lin, Y. Zhao, M. Goto, P.C. Yang, S.-C. Kuo, H.W. Chen, K.-H. Lee, Bioorg. Med. Chem. 23 (2015) 1507–1514.
[16] L. Lin, Q. Shi, C.-Y. Su, C.C.-Y. Shih, K.-H. Lee, Bioorg. Med. Chem. 14 (2006) 2527–2534.
[17] L. Lin, Q. Shi, A.K. Nyarko, K.F. Bastow, C.-C. Wu, C.-Y. Su, C.C.-Y. Shih, K.-H. Lee, J. Med. Chem. 49 (2006) 3964–3972.
[18] J. Wang, M. Sanchez-Rosello, J.L. Acena, C. del Pozo, A.E. Sorochinsky, S. Fustero, V.A. Soloshonok, H. Liu, Chem. Rev. 114 (2014) 2432–2506.
[19] H.-J. Bohm, D. Banner, S. Bendels, M. Kansy, B. Kuhn, K. Muller, U. Obst-Sander, M. Stahl, ChemBioChem 5 (2004) 637–643.
[20] E.V. Rao, P. Sudheer, Indian J. Pharm. Sci. 73 (2011) 262–270.
[21] S. Elavarasan, D. Bhakiaraj, T. Elavarasan, M. Gopalakrishnan, J. Chem. (2013) 1–8, doi:http://dx.doi.org/10.1155/2013/640936.
[22] (a) S. Padhye, H. Yang, A. Jamadar, Q.C. Cui, D. Chavan, K. Dominiak, J. McKinney, S. Banerjee, Q.P. Dou, F.H. Sarkar, Pharm. Res. 26 (2009) 1874–1880; (b) S. Padhye, S. Banerjee, D. Chavan, S. Pandye, K.V. Swamy, S. Ali, J. Li, Q.P. Dou, F.H. Sarkar, Pharm. Res. 26 (2009) 2438–2445.
[23] (a) K. Kamada, S. Senatore, C. Metthews, P.-F. Lenne, O. Maury, C. Andraud, M. Ponce-Vargas, B. Le Guennic, D. Jacquemin, P. Agbo, D.D. An, S.S. Gauny, X. Liu, R.J. Abergel, F. Fages, A. D'Aleo, Chem. Eur. J. 22 (2016) 5219–5232; (b) G. Bai, C. Yu, C. Cheng, E. Hao, Y. Wei, X. Mu, L. Jiao, Org. Biomol. Chem. 12 (2014) 1618–1626.
[24] A.S. Reddy, K.K. Laali, Tetrahedron Lett. (2015) 5495–5499.
[25] M.G. Shioorkar, M.B. Ubale, S.A. Jadhav, R.K. Pardeshi, Der Chemie Sinica 6 (2015) 110–113.
[26] S. Raghavan, P. Manogaran, K.K.G. Narasimha, B.K. Kuppusami, P. Mariyappan, A. Gopalakrishnan, G. Venkatraman, Bioorg. Med. Chem. Lett. 25 (2015) 3601–3605.
[27] J. Chen, Z. Huang, C. Wang, S. Porter, B. Wang, W. Lie, H.K. Liu, Chem. Commun. 51 (2015) 9809–9812.
[28] N. Iqbal, N. Iqbal, Mol. Biol. Int. 2014 (2014) 852748.
[29] S. Xu, R.E. Evans, T. Liu, G. Zhang, J.N. Demas, C.O. Trindle, C.L. Fraser, Inorg. Chem. 52 (2013) 3597–3610.
[30] R.N. Khaybullin, M. Zhang, J. Fu, X. Liang, T. Li, A.R. Katritzky, P. Okunieff, X. Qi, Molecules 19 (2014) 18676–18689.
[31] APEX II, Analytical X-ray Systems, Bruker AXS, Inc., 5465 East Cheryl Parkway, Madison WI, 2005, pp. 53711–55373.
[32] SAINT Version 6.45A, Analytical X-ray Systems, Bruker AXS, Inc., 5465 East Cheryl Parkway, Madison WI, 2003, pp. 53711–55373.
[33] G.M. Sheldrick, SHELXT Acta Cryst. A71 (2015) 3–8.
[34 SHELXTL V6.12, Analytical X-ray Systems, Bruker AXS, Inc., 5465 East Cheryl Parkway, Madison WI, 2002, pp. 53711–55373.
[35] K. Brandenburg, DIAMOND, Crystal Impact GbR, Bonn, Germany, 1999.
[36] (a) A.D. Becke, J. Chem. Phys. 98 (1993) 5648–5652; (b) C. Lee, W. Yang, R.G. Parr, Phys. Rev. B 37 (1988) 785–789; (c) B. Miehlich, B.A. Savin, H. Stoll, H. Preuss, Chem. Phys. Lett. 57 (1989) 200–206.
[37] M.J. Frisch, G.W. Trucks, H.B. Schlegel, G.E. Scuseria, M.A. Robb, J.R. Cheeseman, G. Scalmani, V. Barone, B. Mennucci, G.A. Petersson, et al., Gaussian 09, Gaussian, Inc, Wallingford, CT, 2009.
[38] G.M. Morris, R. Huey, W. Lindstrom, M.F. Sanner, R.K. Belew, D.S. Goodsell, A.J. Olson, J. Comput. Chem. 30 (2009) 2785–2791.
[39] O. Trott, O.A.J. Olson, J. Comput. Chem. 31 (2010) 455–461.
[40] K. Aertgeerts, R. Skene, J. Yano, B.-C. Sang, H. Zou, G. Snell, A. Jennings, K. Iwamoto, N. Habuka, A. Hirokawa, T. Ishikawa, T. Tanaka, H. Miki, Y. Ohta, S.J. Sogabe, J. Biol. Chem. 286 (2011) 18756–18765.
[41] C. Blackburn, C. Barrett, J.L. Blank, F.J. Bruzzese, N. Bump, L.R. Dick, P. Fleming, K. Garcia, P. Hales, Z. Hu, M. Jones, J.X. Liu, D.S. Sappal, M.D. Sintchak, C. Tsu, K. M. Gigstad, Bioorg. Med. Chem. Lett. 20 (2010) 6581–6586.